

**Electronic Supplementary Information (ESI)**

**Low Band Gap Semiconducting Covalent Organic Framework Films with  
Enhanced Photocatalytic Hydrogen Evolution**

Samrat Ghosh,<sup>\*abc</sup> Hüseyin Küçükkeçeci,<sup>c</sup> Rajendra Prasad Paitandi,<sup>d</sup> Vincent Weiget,<sup>c</sup> Veit Dippold,<sup>c</sup> Shu Seki,<sup>\*d</sup> and Arne Thomas,<sup>\*c</sup>

a. Inorganic and Physical Chemistry Laboratory, Council of Scientific and Industrial Research (CSIR), Central Leather Research Institute (CLRI), Chennai-600020, India.

b. Academy of Scientific and Innovative Research (AcSIR), Ghaziabad-201002, India.

c. Department of Chemistry/Functional Materials, Technische Universität Berlin, Berlin 10623, Germany.

d. Department of Molecular Engineering, Graduate School of Engineering, Kyoto University, Nishikyo-ku, Kyoto 615-8510, Japan.

**E-mail:** samrat@clri.res.in

### **Structural Modelling & DFT calculation:**

Geometrical optimization for all the COFs were performed using Materials Studio (2018) software package.<sup>1</sup> Initially, smallest repeating unit of the COF was placed in a crystal cell with P1 symmetry and geometric optimizations were performed using self-consistent-charge (SCC) density functional tight binding method (DFBT+).<sup>2-5</sup> Geometrical optimization was performed using smart algorithm, which is a cascade of the steepest descent, ABNR (adjusted basis set Newton–Raphson), and quasi–Newton methods. Universal force field (UFF)-based Lennard–Jones dispersion corrections was used for the calculation.<sup>6,7</sup> The 3ob parameters was used from the Slater–Koster library and SCC convergence tolerance set at  $1 \times 10^{-8}$ .<sup>8</sup> Divide and conquer was used as the eigensolver. For all the COFs, AA stacks were considered by creating corresponding unit cells and their geometry were optimized, followed by the imposition of high symmetry. Simulated powder diffraction patterns and refinements of PXRD pattern were calculated using Reflex module of Material studio. The density functional theory (DFT) calculations for the small repeating units were carried out using B3LYP function and 6–31g\* as the basis in the Gaussian09 suite (Revision D.01).<sup>9</sup>

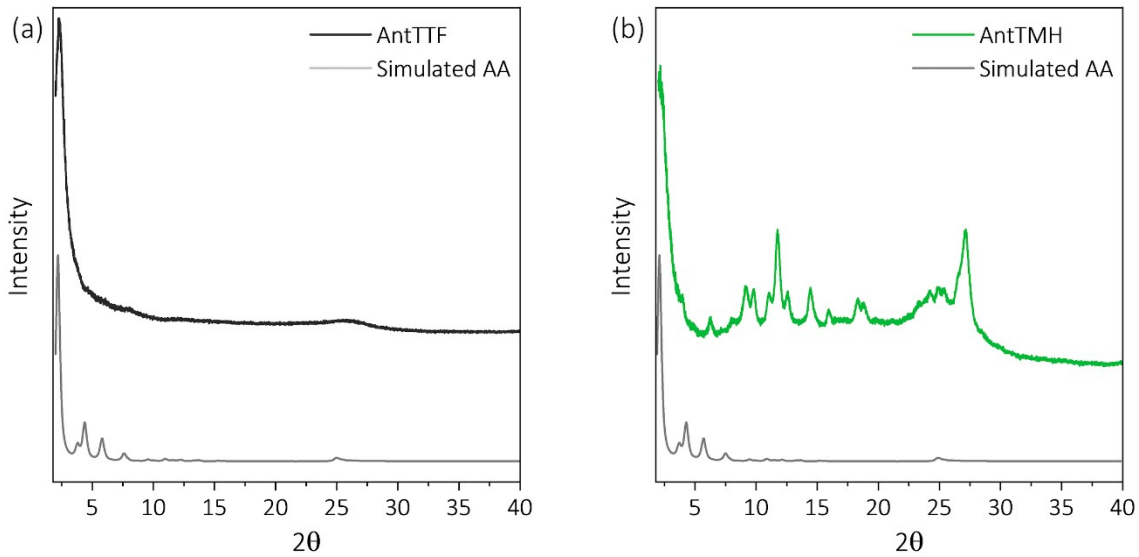


**Fig. S1** Experimental and simulated PXRD of (a) **AntTTF** and (b) **AntTMH**.

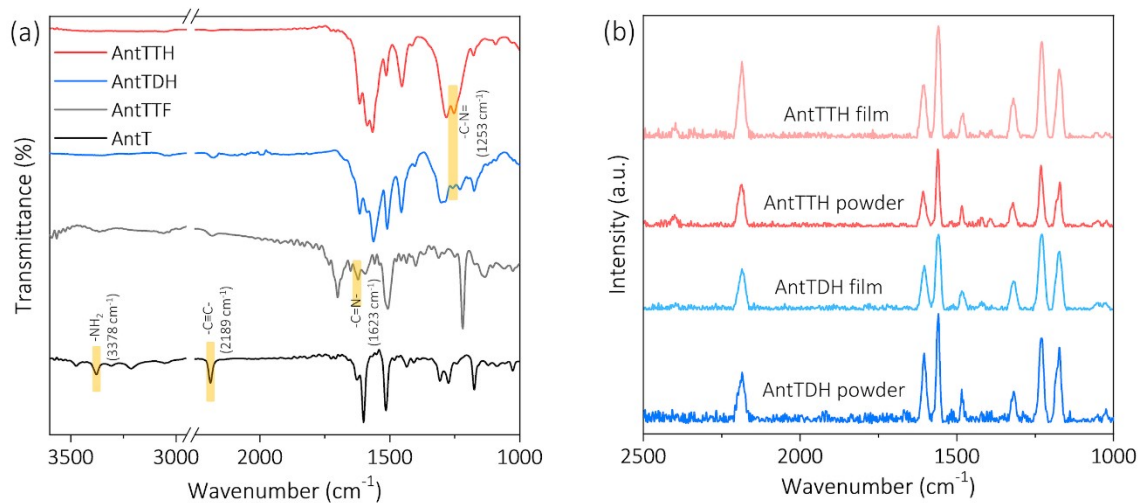


**Fig. S2** (a) FT-IR spectra of **AntTTH**, **AntTDH** and **AntTTF** powders and compared with building block **AntT**. (b) The Raman spectre of powder and film samples of **AntTTH** and **AntTDH**.

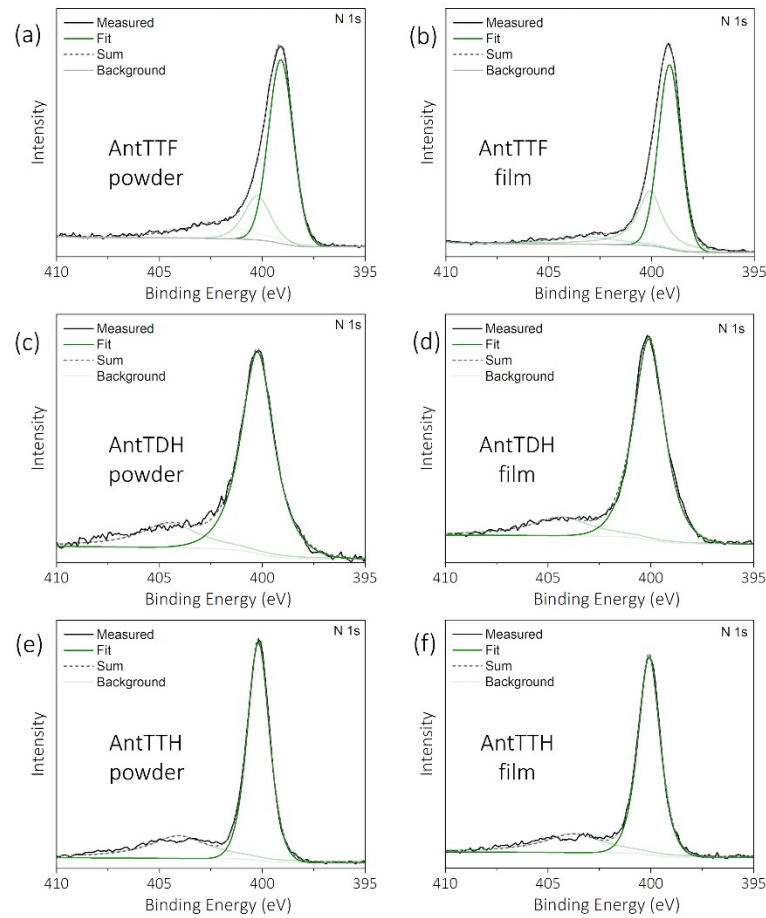


**Fig. S3** N 1s XPS spectra of powder and film sample of (a, b) **AntTTF**, (c, d) **AntTDH** and (e, f) **AntTTH**.

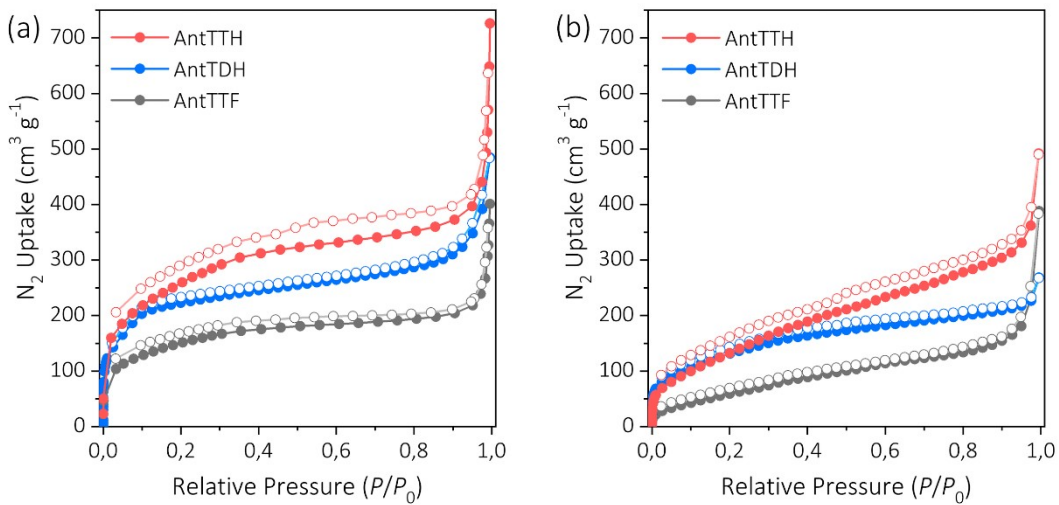


**Fig. S4** Nitrogen sorption isotherms at 77 K for (a) powders and (b) films of **AntTTH**, **AntTDH** and **AntTTF**.

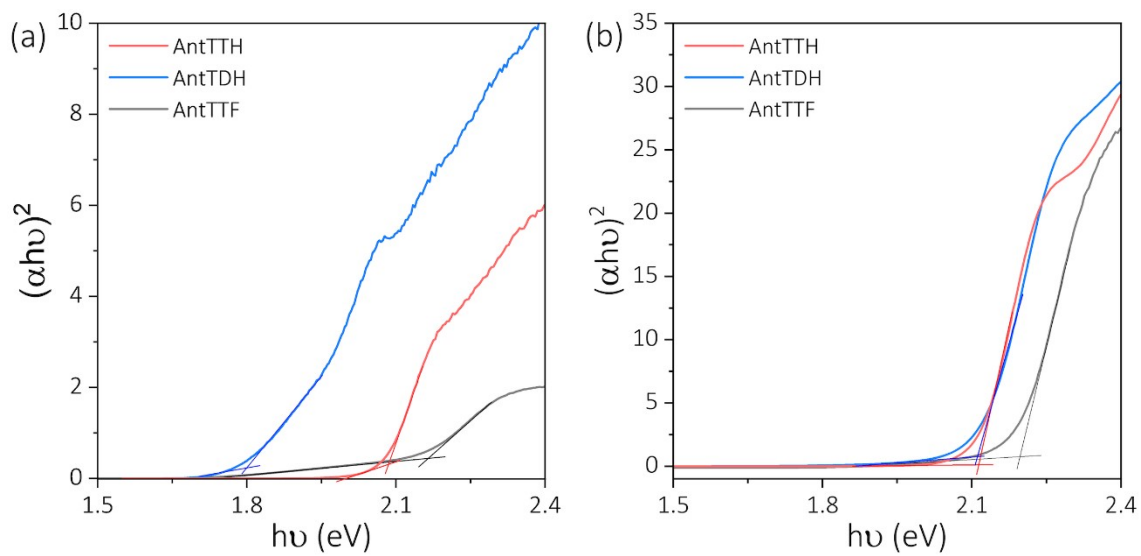


**Fig. S5** The Tauc plots of the (a) powders and (b) films of **AntTTH**, **AntTDH** and **AntTTF**.

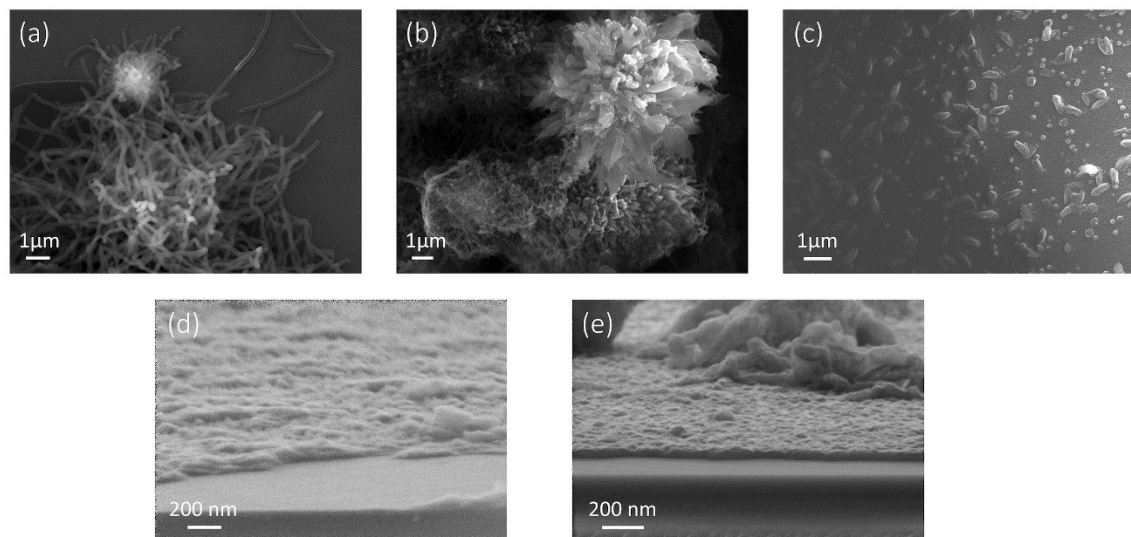


**Fig. S6** SEM images of the (a) **AntTTH**, (b) **AntTDH** and (c) **AntTTF** powders. SEM images of (d) **AntTTH** and (e) **AntTDH** films.

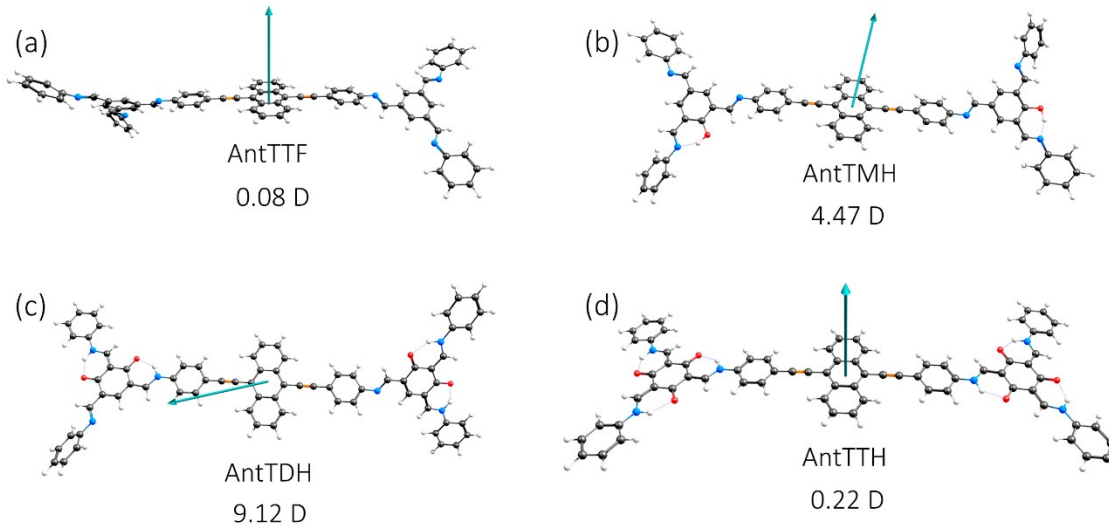


**Fig. S7** Theoretically calculated dipole moment of the energy optimized smallest repeating of (a) **AntTTF**, (b) **AntTMH**, (c) **AntTDH** and (d) **AntTTH** with corresponding value of dipole moment expressed in Debye (D).

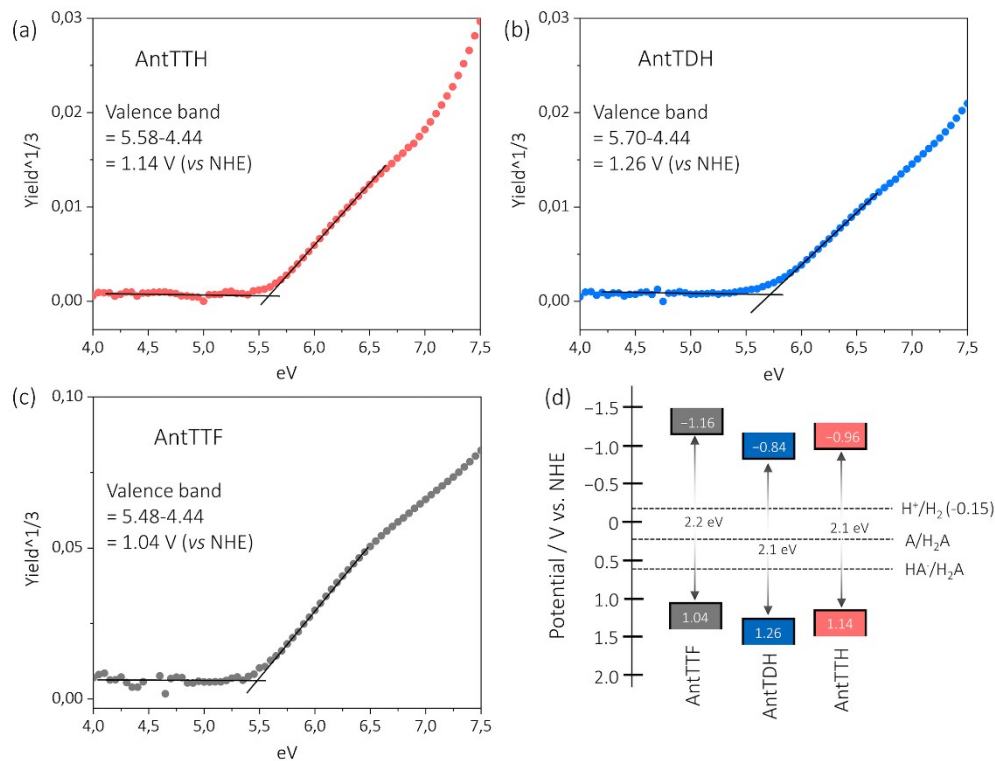


**Fig. S8** Photoelectron yield spectroscopy (PYS) spectra of (a) **AntTTH**, (b) **AntTDH** and (c) **AntTTF**. (d) Calculated band position and band gap of the COF films vs normal hydrogen electrode (NHE) along with the potential of H<sup>+</sup>/H<sub>2</sub> and oxidation potentials of L-ascorbic acid, HA<sup>·</sup>/H<sub>2</sub>A and A/H<sub>2</sub>A and pH 2.6.

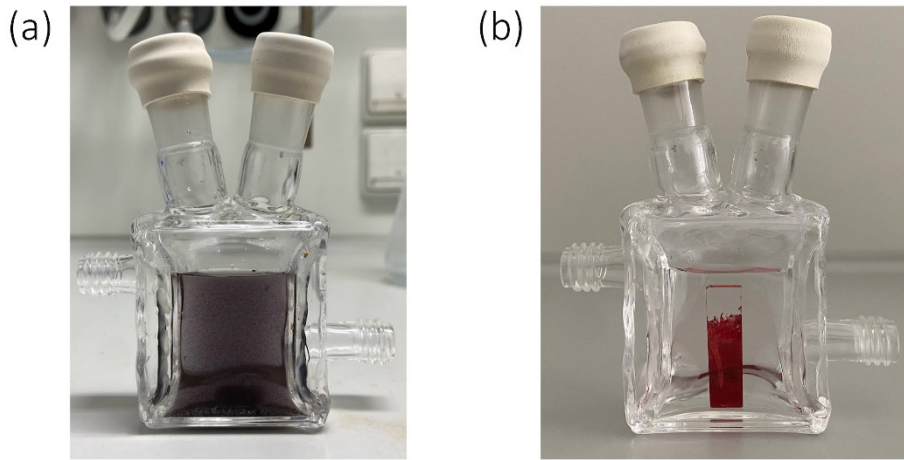


**Fig. S9** Photograph of the photocatalytic reactor containing (a) **AntTDH** powder dispersion and (b) **AntTTH** film over quartz in 16 ml 0.1 M L-ascorbic acid under normal light.

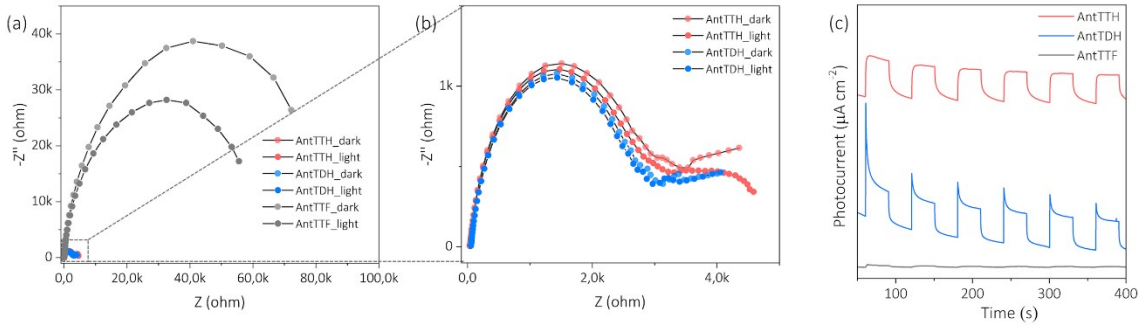


**Fig. S10** (a, b) EIS Nyquist plots and (c) transient photocurrent response of all the COFs under dark and light illumination ( $\geq 420$  nm) at pH 2.6.

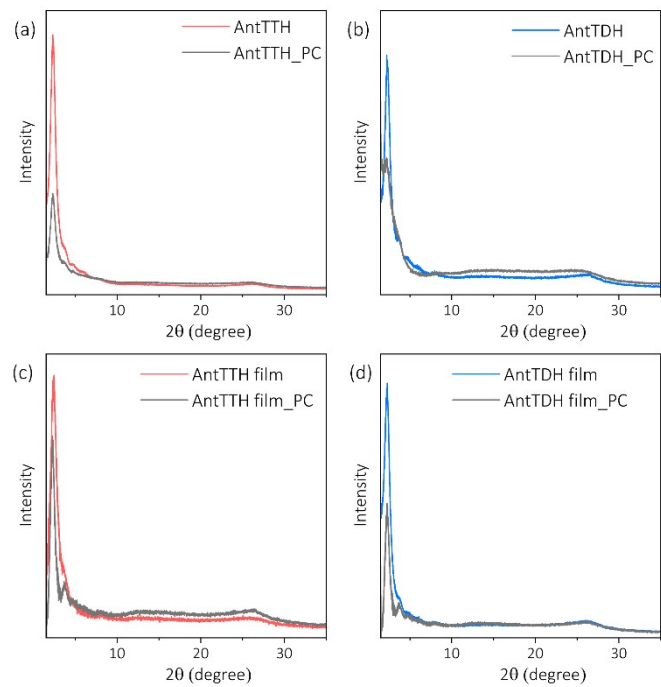


**Fig. S11** Experimental PXRD of the (a,b) powders and (c,d) films before and after the photocatalysis (PC) under visible light for 24 h in 0.1 M ascorbic acid aqueous solution at pH 2.6 using platinum as the co-catalyst.

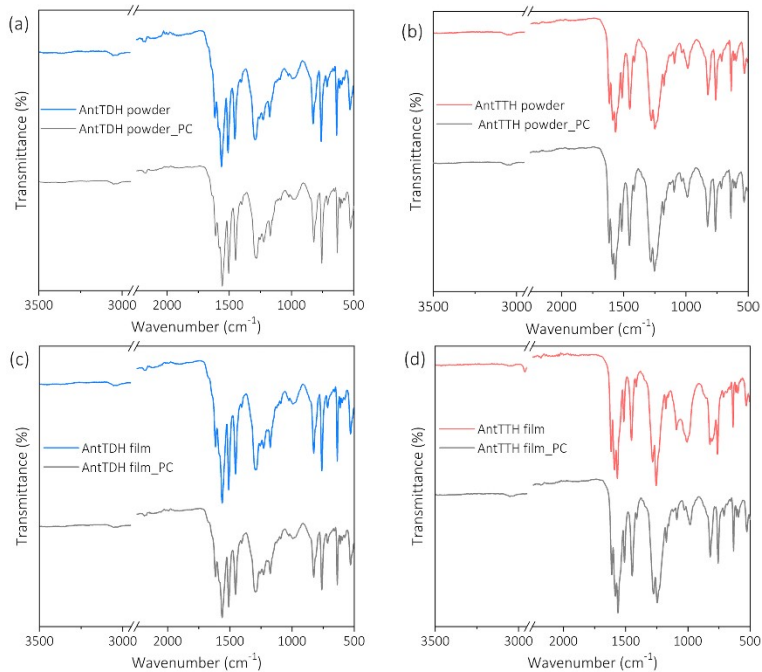


**Fig. S12** FT-IR spectra of the (a,b) powders and (c,d) films before and after the photocatalysis (PC) under visible light for 24 h in 0.1 M ascorbic acid aqueous solution at pH 2.6 using platinum as the co-catalyst.

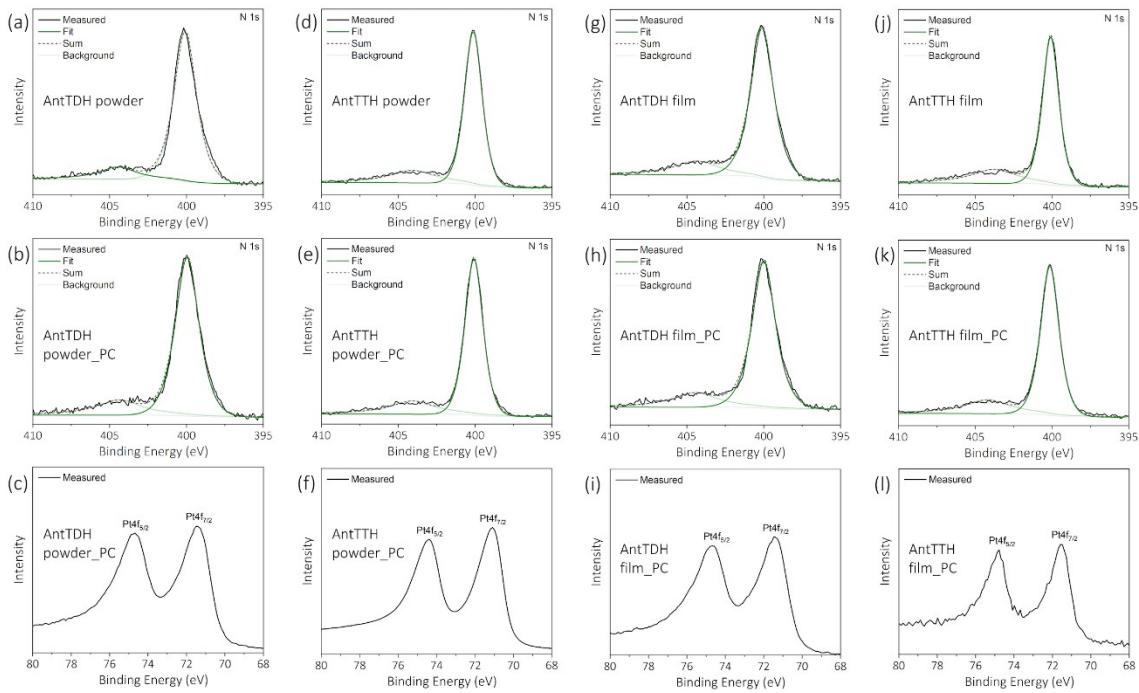


**Fig. S13** XPS of the (a,b) powders and (c,d) films before and after the photocatalysis (PC) under visible light for 24 h in 0.1 M ascorbic acid aqueous solution at pH 2.6 using platinum as the co-catalyst.

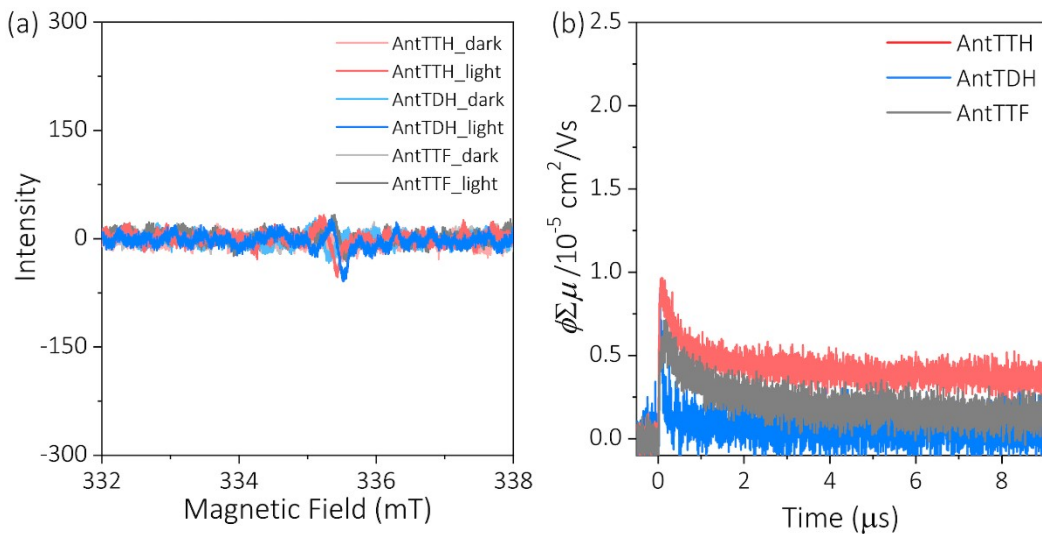


**Fig. S14** (a) Change in EPR signal of pristine COF powders under light and dark. (b) Photoconductivity transients of COF powders under 355 nm laser excitation.

## References:

1. Materials Studio, BIOVIA Software Inc., San Diego, CA, (2018).
2. B. Hourahine, B. Aradi, V. Blum, F. Bonafé, A. Buccheri, C. Camacho, C. Cevallos, M. Y. Deshaye, T. Dumitrică, A. Dominguez, S. Ehlert, M. Elstner, T. van der Heide, J. Hermann, S. Irle, J. J. Kranz, C. Köhler, T. Kowalczyk, T. Kubář, I. S. Lee, V. Lutsker, R. J. Maurer, S. K. Min, I. Mitchell, C. Negre, T. A. Niehaus, A. M. N. Niklasson, A. J. Page, A. Pecchia, G. Penazzi, M. P. Persson, J. Řezáč, C. G. Sánchez, M. Sternberg, M. Stöhr, F. Stuckenbergs, A. Tkatchenko, V. W.-z. Yu and T. Frauenheim, *J. Chem. Phys.*, 2020, **152**, 124101.
3. M. Gaus, Q. Cui and M. Elstner, *J. Chem. Theory Comput.*, **2011**, *7*, 931–948.
4. B. Lukose, A. Kuc and T. Heine, *Chem. – Eur. J.*, **2011**, *17*, 2388–2392.
5. B. Aradi, B. Hourahine and T. Frauenheim, *J. Phys. Chem. A*, 2007, **111**, 5678–5684.
6. A. K. Rappe, C. J. Casewit, K. S. Colwell, W. A. Goddard III and W. M. Skiff, *J. Am. Chem. Soc.*, **1992**, *114*, 10024–10035.
7. A. K. Rappe, C. J. Casewit, K. S. Colwell, W. A. Goddard III and W. M. Skiff, *J. Am. Chem. Soc.*, **1992**, *114*, 10035–10046.
8. M. Gaus, A. Goez and M. Elstner, Parametrization and Benchmark of DFTB3 for Organic Molecules, *J. Chem. Theory Comput.*, 2012, **9**, 338–354.
9. Gaussian 09, Revision D.01, M. J. Frisch, G. W. Trucks, H. B. Schlegel, G. E. Scuseria, M. A. Robb, J. R. Cheeseman, G. Scalmani, V. Barone, B. Mennucci, G. A. Petersson, H. Nakatsuji, M. Caricato, X. Li, H. P. Hratchian, A. F. Izmaylov, J. Bloino, G. Zheng, J. L. Sonnenberg, M. Hada, M. Ehara, K. Toyota, R. Fukuda, J. Hasegawa, M. Ishida, T. Nakajima, Y. Honda, O. Kitao, H. Nakai, T. Vreven, J. A. Montgomery, Jr., J. E. Peralta, F. Ogliaro, M. Bearpark, J. J. Heyd, E. Brothers, K. N. Kudin, V. N. Staroverov, R. Kobayashi, J. Normand, K. Raghavachari, A. Rendell, J. C. Burant, S. S. Iyengar, J. Tomasi, M. Cossi, N. Rega, J. M. Millam, M. Klene, J. E. Knox, J. B. Cross, V. Bakken, C. Adamo, J. Jaramillo, R. Gomperts, R. E. Stratmann, O. Yazyev, A. J. Austin, R. Cammi, C. Pomelli, J. W. Ochterski, R. L. Martin, K. Morokuma, V. G. Zakrzewski, G. A. Voth, P. Salvador, J. J. Dannenberg, S. Dapprich, A. D. Daniels, Ö. Farkas, J. B. Foresman, J. V. Ortiz, J. Cioslowski, and D. J. Fox, Gaussian, Inc., Wallingford CT, 2009.